THE JOURNAL OF BIOLOGICAL CHEMISTRY VOL. 291, NO. 29, pp. 14973–14985, July 15, 2016

Regulation of the Yeast Hxt6 Hexose Transporter by the Rod1 α-Arrestin, the Snf1 Protein Kinase, and the Bmh2 14-3-3 Protein*

Received for publication, April 28, 2016, and in revised form, June 3, 2016 Published, JBC Papers in Press, June 3, 2016, DOI 10.1074/jbc.M116.733923

Vicent Llopis-Torregrosa[‡1,2], Alba Ferri-Blázquez[‡1], Anna Adam-Artigues[‡], Emilie Deffontaines[‡], G. Paul H. van Heusden[§], and Lynne Yenush[‡3]

From the: [‡]Instituto de Biología Molecular y Celular de Plantas (IBMCP), Universitat Politècnica de València-Consejo Superior de Investigaciones Científicas, 46022 Valencia, Spain and the [§]Section Molecular and Developmental Genetics, Institute of Biology, Leiden University, Sylviusweg 72, 2333BE Leiden, The Netherlands

Cell viability requires adaptation to changing environmental conditions. Ubiquitin-mediated endocytosis plays a crucial role in this process, because it provides a mechanism to remove transport proteins from the membrane. Arrestin-related trafficking proteins are important regulators of the endocytic pathway in yeast, facilitating selective ubiquitylation of target proteins by the E3 ubiquitin ligase, Rsp5. Specifically, Rod1 (Art4) has been reported to regulate the endocytosis of both the Hxt1, Hxt3, and Hxt6 glucose transporters and the Jen1 lactate transporter. Also, the AMP kinase homologue, Snf1, and 14-3-3 proteins have been shown to regulate Jen1 via Rod1. Here, we further characterized the role of Rod1, Snf1, and 14-3-3 in the signal transduction route involved in the endocytic regulation of the Hxt6 high affinity glucose transporter by showing that Snf1 interacts specifically with Rod1 and Rog3 (Art7), that the interaction between the Bmh2 and several arrestin-related trafficking proteins may be modulated by carbon source, and that both the 14-3-3 protein Bmh2 and the Snf1 regulatory domain interact with the arrestin-like domain containing the N-terminal half of Rod1 (amino acids 1–395). Finally, using both co-immunoprecipitation and bimolecular fluorescence complementation, we demonstrated the interaction of Rod1 with Hxt6 and showed that the localization of the Rod1-Hxt6 complex at the plasma membrane is affected by carbon source and is reduced upon overexpression of *SNF1* and *BMH2*.

An important component of the maintenance of cellular homeostasis and stress responses is the regulation of the composition of plasma membrane proteins responsible for the uptake and extrusion of nutrients and other nonpermeable small molecules. The general mechanisms controlling this regulatory process are highly conserved among eukaryotic organisms and involve both transcriptional regulation and modulation of the balance of secretion, recycling, and degradation of individual transporter proteins in response to changes in the extracellular environment (reviewed in Ref. 1). Regulated endocytosis, one important step in this process, has been well studied in both mammals and yeast, unveiling many mechanistic similarities that establish yeast as a relevant model system.

In *Saccharomyces cerevisiae*, plasma membrane transporters that need to be down-regulated are ubiquitylated by the Rsp5 E3 ubiquitin ligase, endocytosed, sorted into multivesicular bodies in a process requiring the ESCRT machinery, and finally are delivered to the vacuole for degradation (2–5). Transporter ubiquitylation by the HECT family Rsp5 E3 ubiquitin ligase is mediated by one or more of several adaptor proteins that confer specificity and ensure the correct regulation of targeted proteins in response to changes in the extracellular environment (reviewed in Refs. 6). At least 18 Rsp5 adaptor proteins have been described, each having specificity for a subset of transport proteins and acting in response to specific stimuli.

The molecular mechanisms governing these regulatory interactions are beginning to be clarified. For example, one subset of the Rsp5 adaptor proteins shows structural conservation and has been assigned to the arrestin-related trafficking (ART)[4] adaptor family (7). The 14 members of this protein family contain a conserved fold in their N terminus that shows structural homology to the mammalian α and β arrestins and 1–3 repeats of the Rsp5 binding (L/P)P*X*Y motif (8). In yeast, physical interactions have been demonstrated between Rsp5 adaptors Ecm21 (Art2) and Aly2 (Art3) with the Smf1 divalent metal cation transporter and the Dip5 aspartic acid permease, respectively (9, 10). In the case of Dip5, addition of excess substrate was shown to increase the interaction with Aly2, whereas in the case of Ecm21, no alterations in Smf1 interaction were observed. Importantly, where within the cell these protein-protein interactions take place has not been extensively studied. In other cases, genetic evidence supports a role for the requirement for Rsp5 adaptors for the down-regulation of defined transporters but direct proof of physical interactions has not yet been reported (7, 11).

The endocytic activity of Rsp5 adaptor proteins has been shown to be modulated by protein phosphorylation/dephos-

* This work was supported by Grant BFU2011-30197-C03-03 from the Ministerio de Economía y Competitividad (Madrid, Spain) and in part by Netherlands Organization for Scientific Research-Earth and Life Sciences Grant 826.09.006. The authors declare that they have no conflicts of interest with the contents of this article.

[1] Both authors contributed equally to this work.

[2] Supported by a predoctoral fellowship from the Polytechnic University of Valencia.

[3] To whom correspondence should be addressed: Instituto de Biología Molecular y Celular de Plantas, c/ de Vera s/n, 46022 Valencia, Spain. Tel.: 34-963879375; Fax: 34-963877879; E-mail: lynne@ibmcp.upv.es.

[4] The abbreviations used are: ART, arrestin-related trafficking protein; BiFC, bimolecular fluorescence complementation; TGN, trans-Golgi network.

phorylation switches in several cases. The first example was modulation of the activity of Ldb19(Art1) by the TORC1-responsive kinase, Npr1. Hyperphosphorylation of Ldb19 by Npr1 was shown to inhibit its endocytic activity for the Can1 arginine permease (12). The Npr1 kinase was also shown to inhibit the endocytic activity of the Bul1 and Bul2 Rsp5 adaptors by creating binding sites for 14-3-3 proteins, which then impede the degradation of the Gap1 general amino acid permease, presumably by preventing the association of the Rsp5-adaptor complex with Gap1 (13). In this case, the Sit4 phosphatase has been proposed to be involved in Bul1 and Bul2 dephosphorylation, leading to their activation and subsequent down-regulation of Gap1 under the appropriate conditions, although direct dephosphorylation of Bul1 and Bul2 by Sit4 was not demonstrated. In addition, the calcineurin phosphatase was shown to directly dephosphorylate another Rsp5 adaptor Aly2, promoting its endocytic activity for Dip5, but not for Gap1 (14). These studies show that complex regulatory routes are employed to fine-tune the cohort of transport proteins present in the plasma membrane in response to the quality of the nitrogen source.

The Rsp5 adaptor network has also been shown to respond to changes in the carbon source. On one hand, Rod1 was shown genetically to be involved in the down-regulation of the Hxt6 high affinity glucose permease and was also implicated in the endocytosis of the Hxt1 and Hxt3 transporters in response to 2-deoxyglucose (11, 15). This adaptor was also shown to regulate the Rsp5-mediated ubiquitylation of the Jen1 lactate transporter in response to glucose addition and the Ste2 pheromone receptor (16–18). In the report studying Jen1 regulation, the Snf1 kinase, which was previously shown to phosphorylate Rod1 (19), was shown to create binding sites for the 14-3-3 proteins. Similar to what was observed for Bul1 and Bul2, 14-3-3 binding to Rod1 was shown to impede Jen1 delivery and subsequent degradation in the vacuole. In both cases, 14-3-3 binding to the Rsp5 adaptor is postulated to block the interaction with the targeted transporter, although this has not been experimentally proven.

In the present study, we aimed to further characterize the signal transduction route involved in the endocytic regulation of the Hxt6 high affinity glucose transporter. We show that the Snf1 kinase interacts physically with both the Rod1 Rsp5 adaptor protein and with the closely related Rog3 adaptor, but not with other ART family members. We also show that the 14-3-3 protein Bmh2 interacts with many ART family members, suggesting a general role for these proteins in the Rsp5 signaling network. Moreover, we show that Rod1 physically interacts with Hxt6 principally at the plasma membrane. Upon overexpression of either *SNF1* or *BMH2*, the Rod1-Hxt6 complex is present, but a lower percentage of the signal is observed at the plasma membrane. Accordingly, glucose-induced Hxt6 degradation is delayed in these strains. Finally, we also demonstrate the interaction between Rod1 and Hxt1. Thus, our work provides experimental proof of the physical interaction *in vivo* between an ART family member and its cargo proteins, which shows specificity both at the level of environmental stimulus and subcellular localization.

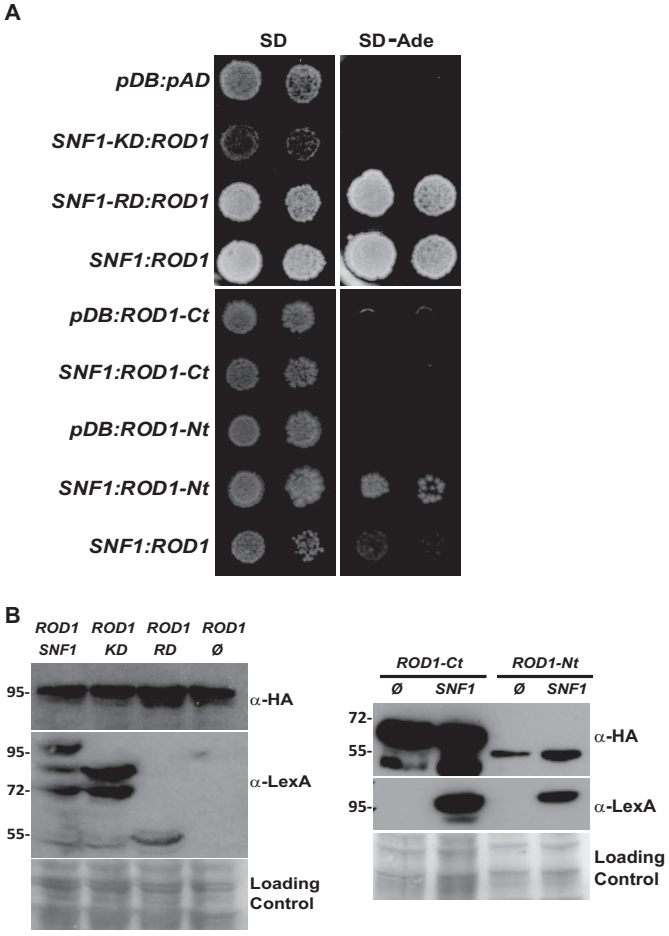

FIGURE 1. **Mapping of the domains required for the interaction between Snf1 and Rod1.** *A*, strains transformed with plasmids containing the full-length *SNF1* gene, the kinase domain (amino acids 1–391, *SNF1-KD*) or the regulatory domain (amino acids 392–633, *SNF1-RD*) fused to the LexA DNA-binding domain and the full-length *ROD1*, the arrestin domain-containing N terminus (amino acids 1–395, *ROD1*-Nt) or the (L/P)PXY motif-containing C terminus (amino acids 396–837, *ROD1*-Ct) fused to the Gal4 activation domain were grown to saturation in selective medium, serially diluted, and spotted onto plates with the indicated composition. Growth was recorded after 48–72 h. Identical results were obtained for three independent transformants. *B*, correct expression of all proteins in whole cell extracts was confirmed by immunodetection using the indicated antibodies. Molecular weight markers are indicated on the *left*, and direct blue staining of the membrane is shown in the *bottom panel* as the loading control.

Results

The Snf1 kinase was previously reported to phosphorylate the ART family protein, Rod1 (19). We tested whether these two proteins physically interact in a yeast two-hybrid assay. As shown in Fig. 1, we not only detected this interaction but also mapped the regions of these proteins required for the interaction. We show that the regulatory domain of Snf1 (Snf1-RD) interacts with the N-terminal half of Rod1, which contains the arrestin-like domain. Interestingly, this is also the domain of Rod1 implicated in binding the protein phosphatase regulatory subunit, Reg1 (16).

We further analyzed whether this interaction was specific for Rod1 or whether other ART family members also interacted with Snf1 in this assay. As shown in Fig. 2, Snf1 interacts only with Rod1 and the closely related Rog3 (Art7) protein. No growth was observed in control strains co-transformed with the

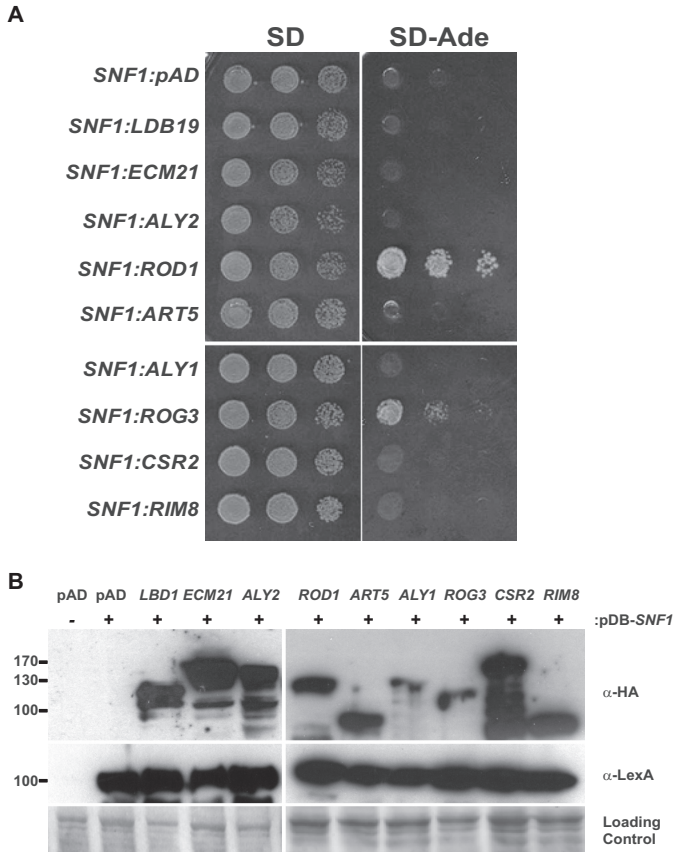

FIGURE 2. **Snf1 interacts with Rod1 and Rog3 but not with other ART family members.** *A*, strains transformed with plasmids containing the full-length *SNF1* gene fused to the LexA DNA-binding domain and nine ART family member genes fused to the Gal4 activation domain were grown to saturation in selective medium, serially diluted, and spotted onto plates with the indicated composition. Growth was recorded after 48–72 h. Identical results were obtained for three independent transformants. No growth was observed in empty vector controls expressing the ART proteins (not shown). *B*, correct expression of the fusion proteins was confirmed by Western blotting as described in Fig. 1*B*.

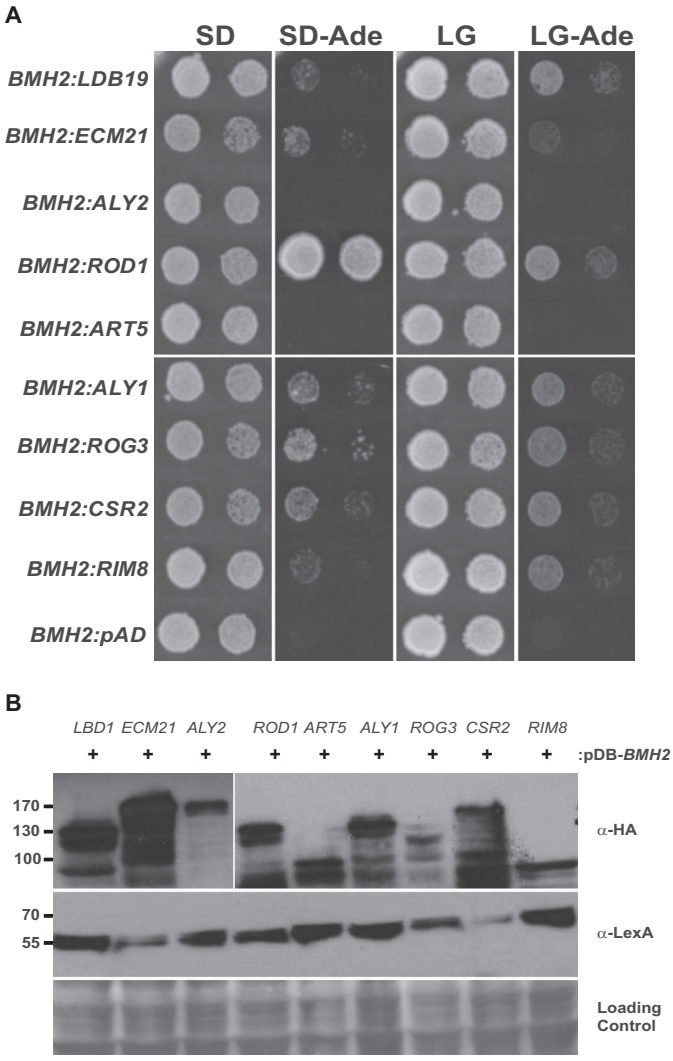

FIGURE 3. **The 14-3-3 protein Bmh2 physically interacts with several ART family members.** *A*, strains transformed with plasmids containing the *BMH2* gene fused to the LexA DNA-binding domain, and nine ART family member genes fused to the Gal4 activation domain were grown to saturation in selective medium, serially diluted, and spotted onto plates with the indicated composition. Growth was recorded after 48–72 h. Identical results were obtained for three independent transformants. *B*, correct expression of the fusion proteins was confirmed by Western blotting as described in Fig. 1*B*.

ART vectors and the empty LexA-containing vector (data not shown). Our results support previous reports showing a functional interaction between Rod1 and Snf1 and show that Rog3 may also be regulated in a similar way (16, 19). Moreover, they suggest that Snf1 is not a general regulator of ART family proteins and support the idea of a partitioning of the functions of Rsp5 adaptor proteins to respond to different classes of environmental changes through protein phosphorylation by specific kinases, such as those related to carbon (Snf1-Rod1/Rog3) or nitrogen (Npr1-Art1) sources (12, 16).

Based on previous data in mammals implicating a role for 14-3-3 proteins in the regulation of the Rsp5 orthologue, Nedd4.2 (20, 21), we tested whether the WW domains of Rsp5 physically interact with the yeast 14-3-3 protein Bmh2. Because we did not detect binding in this assay (data not shown) and recent reports and high throughput studies show that 14-3-3 proteins interact with Rsp5 adaptor proteins (13, 16), we performed a yeast two-hybrid analysis of Bmh2 with 9 ART family members to assay this interaction under different experimental conditions. As shown in Fig. 3, all ART family proteins except Aly2 (Art3) and Art5 interacted with Bmh2 under the conditions tested. We performed this assay in selective medium containing either 2% glucose (synthetic dextrose (SD) medium) or in low glucose (LG) medium, containing 0.05% glucose, 2% glycerol, 2% galactose, and 2% ethanol as the carbon source, to test responsiveness to this environmental condition (22). Interestingly, we observed that the relative growth pattern differed in these two conditions. Although suggestive, more experiments will be required to establish the physiological relevance of these interactions.

We next studied the interaction between Rod1 and Bmh2 in the presence and absence of *SNF1* overexpression (Fig. 4, *A–D*). We employed *SNF1* mutants harboring point mutants, which constitutively activate (G53R) or deactivate (K84R) the kinase (23). The proposed model suggests that Snf1 phosphorylation of Rod1 creates binding sites for 14-3-3 protein interaction. Accordingly, we should be able to detect differences in yeast two-hybrid interactions by monitoring the activity of β-galactosidase. As shown in Fig. 4*C*, we observe an increase in the

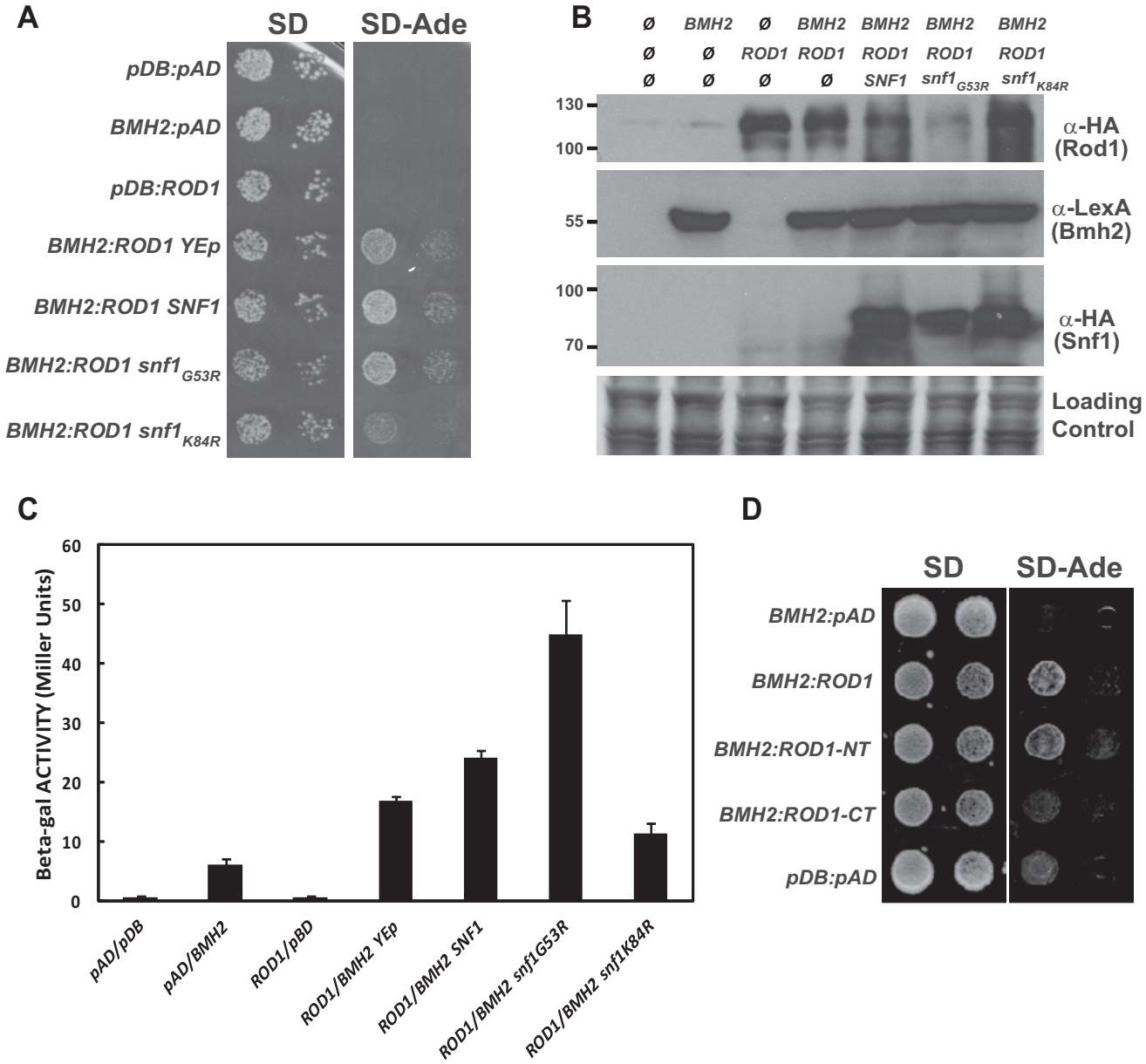

FIGURE 4. **Bmh2 interacts with the Rod1 N terminus and Snf1 kinase activity improves this interaction.** *A*, strains transformed with the indicated plasmids described in Figs. 1 and 3 were analyzed as described. Identical results were observed for three independent transformants. *B*, correct expression of the fusion proteins was confirmed by Western blotting as described in Fig. 1*B*. *C*, the indicated strains were grown to mid-log phase in selective medium, collected by centrifugation, and processed for the determination of β-galactosidase activity, as described under "Experimental Procedures." The data represent the average values of triplicate determinations for three independent transformants. The *error bars* represent the standard deviation. β-Galactosidase activity was undetectable in the controls containing empty plasmids. *D*, the strains transformed with the indicated plasmids were analyzed for protein-protein interactions as described in Fig. 1.

β-galactosidase activity in strains co-expressing *ROD1-AD*/*BMH2-DB* and *SNF1*. Moreover, expression of a mutated version of Snf1 that is constitutively active increases the Rod1-Bmh2 interaction, whereas overexpression of a kinase-dead version of Snf1 shows a similar level of Rod1-Bmh2 interaction as the empty vector control. The growth assays shown in Fig. 4*A* corroborate the data obtained in the β-galactosidase assays. These results complement the existing data used to propose the model presented by Becuwe *et al.* (16) for the regulation of the Jen1 lactate transporter, where they showed a reduction in the amount of Rod1 present in a Bmh2-GST pulldown in strains lacking *SNF1*. Our data show that the kinase activity of Snf1 is required for the increase in Rod1-Bmh2 interaction. Interestingly, we did not see any difference in these assays when we used a mutant form of Rod1 lacking the previously identified Snf1 phosphorylation site at serine 447 (data not shown), suggesting that this assay is not sensitive enough to detect this change or that other phosphorylation sites are also involved in 14-3-3 binding (19). To further clarify this point, we checked the interaction between Bmh2 and the N- and C-terminal parts of Rod1. As shown in Fig. 4*D*, we observed an interaction between Bmh2 and the N-terminal domain of Rod1 (amino acids 1–395), suggesting that that serine 447 is not likely to be the only phosphorylation site involved in the Bmh2-Rod1 interaction.

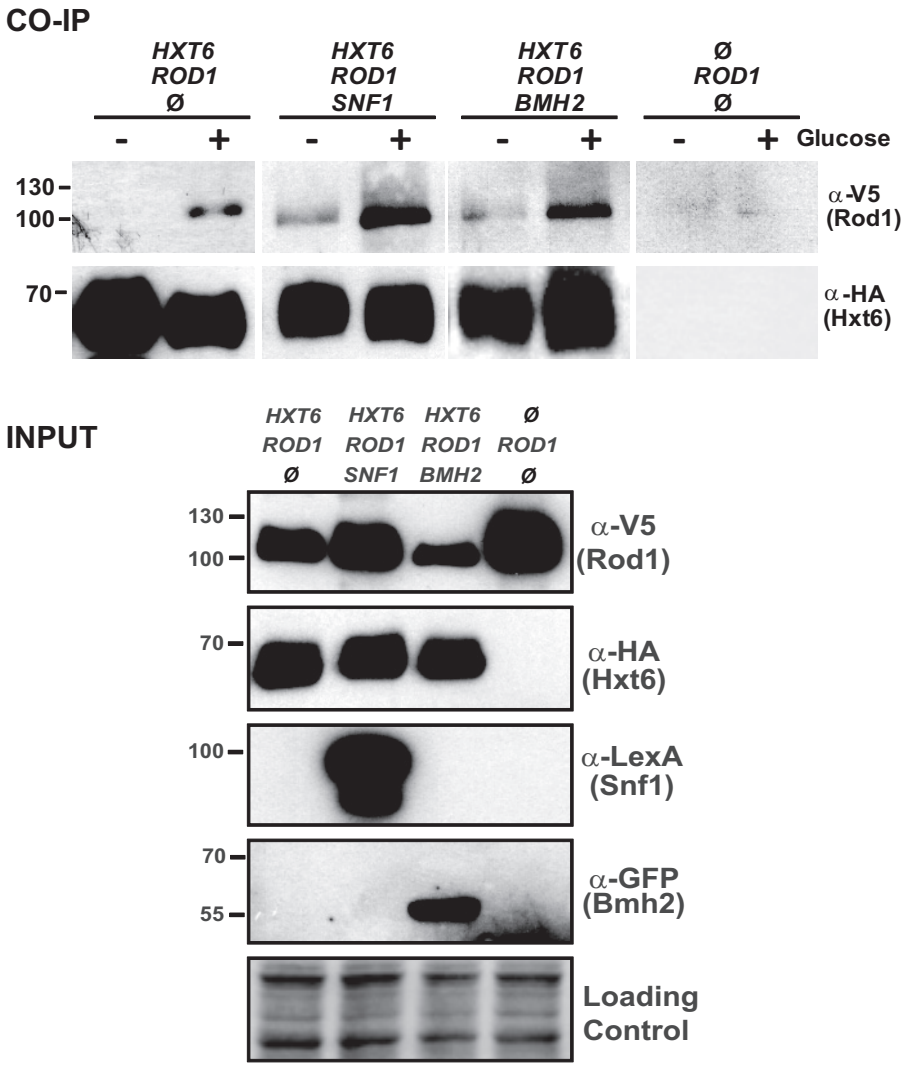

FIGURE 5. **Rod1 co-immunoprecipitates with Hxt6.** The BY4741 strain was transformed with plasmids containing the indicated genes, grown in raffinose-containing medium, treated with glucose for 30 min (final concentration, 2%), and processed for co-immunoprecipitation as described under "Experimental Procedures." The purified proteins were separated on SDS-PAGE gels, transferred to nitrocellulose membranes, and successively analyzed with the indicated antibodies (*upper panels*). The *bottom panels* show the correct expression of fusion proteins in the proteins extracts employed for the co-immunoprecipitation experiments. Molecular weight markers are indicated on the *left*. Similar results were observed in three independent experiments.

We were next interested in studying the physical interaction between Rod1 and the Hxt6 hexose transporter. Previous studies have shown that Rod1 is necessary for the down-regulation of Hxt6 when cells are shifted from raffinose to glucose-containing medium (11). At least two studies have presented different experimental evidence showing that ART family members bind directly to transporter proteins (9, 10). However, in these cases, *in vivo* interactions in live cells were not reported, nor were the subcellular localization of the complexes. Here, we show both by co-immunoprecipitation and bimolecular fluorescence complementation (BiFC) that Rod1 physically interacts with Hxt6 (Figs. 5 and 6). Specifically, in the co-immunoprecipitation experiments, we observe an increase in the amount of Rod1 that binds to Hxt6 in cells treated with glucose for 30 min, as compared with those grown in raffinose. Moreover, we also detect more Rod1 in the Hxt6 immunoprecipitate both before treatment and in glucose-treated cells overexpressing *SNF1* or *BMH2* (Fig. 5).

Using the BiFC assay, which is capable of detecting and determining the subcellular localization of protein-protein interactions in live cells, we demonstrate that a Rod1-Hxt6 complex can be detected principally at the cell surface in cells growing in raffinose as the sole carbon source. Importantly, no fluorescence was detected in either of the control combinations (Hxt6-VC/VN or VC/Rod1-VN; Fig. 6*A*). Using both FM4-64 treatments and co-localization studies with endosomal (FYVE-DsRed) and trans-Golgi network (TGN) (Sec7-DsRed) markers (24), we show that this signal partially co-localizes with endocytic vesicles and the vacuole (Fig. 6, *B–D*). Upon glucose treatment, we observe decrease in the plasma membrane fluorescence/internal fluorescence ratio, consistent with the vacuolar degradation of the complex (Fig. 6*E*). The vacuolar signal observed is likely to be a result of the permanent reconstitution of the Venus protein upon Hxt6-Rod1 interaction. Further studies are required to determine whether Rod1 travels with Hxt6 to the vacuole for

degradation. In any case, to our knowledge these results represent the first observation of the interaction *in vivo* between a yeast α-arrestin and its cargo protein.

We next studied the interaction between Rod1 and the Hxt1 hexose transporter, which was recently identified to be regulated by this α-arrestin in response to 2-deoxyglucose treatment (15). As observed in Fig. 7, the weak Rod1-Hxt1 BiFC signal appears internally independent of the carbon source. No fluorescence was observed with either control combination (Hxt1-VC/VN or VC/Rod1-VN; Fig. 7*A*). Upon 2-deoxyglucose

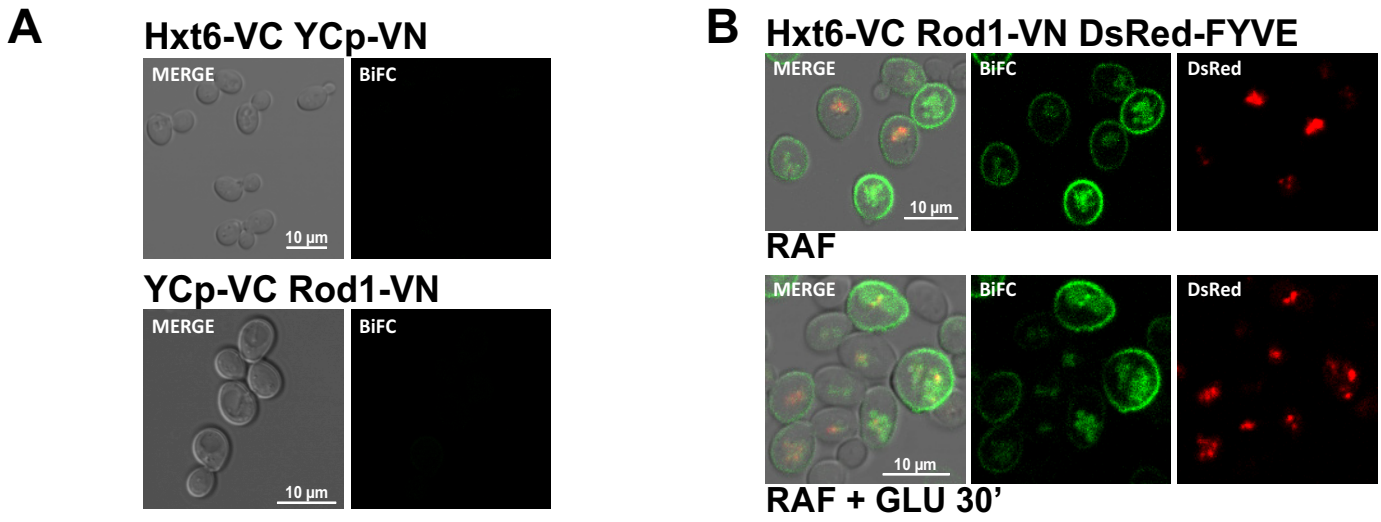

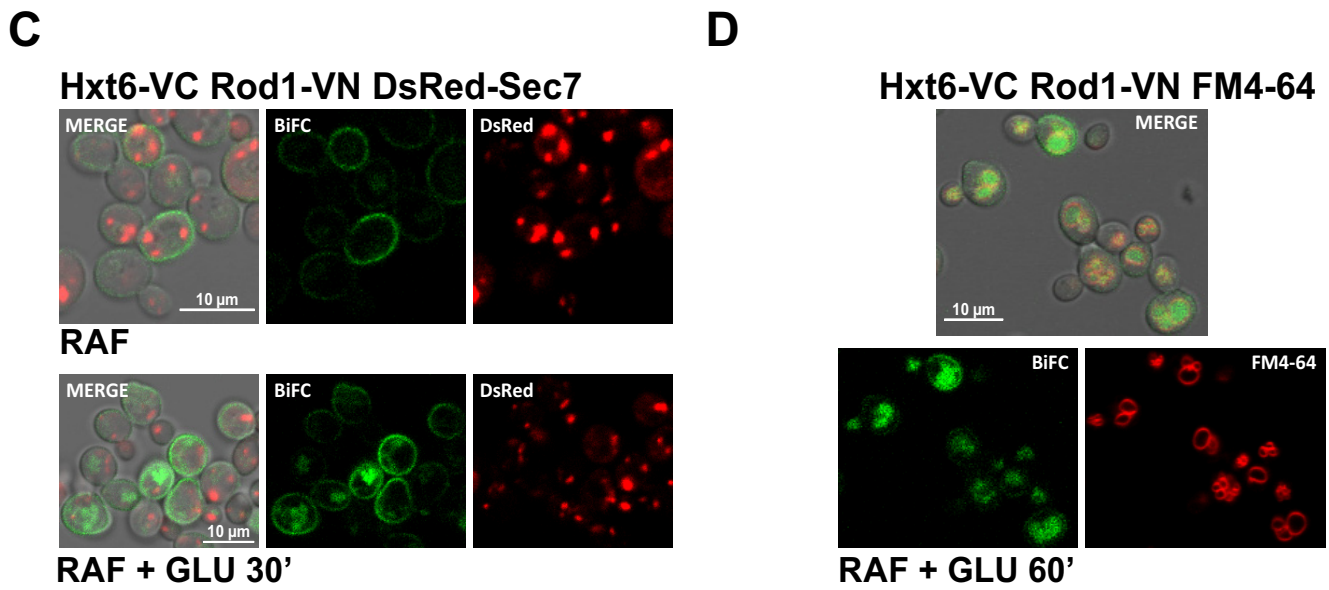

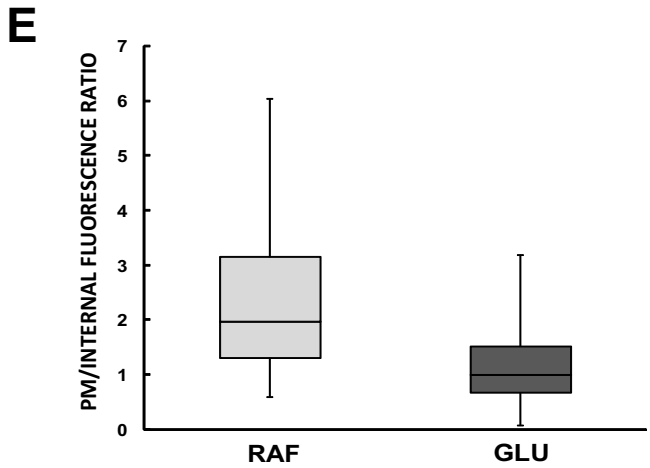

treatment, a strong interaction is detected in punctate structures that co-localize with the FYVE domain containing endocytic marker, but not the Sec7 TGN marker. It is interesting to note that we very rarely observed the interaction at the cell surface regardless of the carbon source or treatments employed, which is in stark contrast to that observed in the case of Hxt6-Rod1. These data suggest additional levels of control of spatial and temporal specificity of the interaction between α-arrestins and their cargo proteins.

Because the BiFC experiments described above for Hxt6-Rod1 were performed with a plasmid-borne version of Rod1, we performed a BiFC analysis with genomically integrated fusion proteins so that both fusion proteins would be under the control of their own promoter. We consider this analysis to be crucial to avoid misinterpretations because of overexpression of the proteins involved in complex formation and because our experiments and previous studies have shown that Rod1 protein accumulation and post-translational modifications are regulated by carbon source (Fig. 8*A* and Refs. 16 and 19). To this end, we quantified the amount of fluorescence observed at the plasma membrane upon glucose treatment of raffinose-grown cells, as described under "Experimental Procedures." Although the signal is much weaker, as would be expected for endogenous expression levels, upon glucose addition, we observe that the majority of the signal corresponding to the Hxt6-Rod1 complex forms at the plasma membrane (Fig. 8, *B* and *C*). These results suggest that under physiological conditions, the Hxt6-Rod1 complex forms at the plasma membrane, presumably facilitating Rsp5-dependent ubiquitylation of Hxt6 upon glucose addition. This result is the experimental confirmation of the model proposed based on indirect evidence by Becuwe *et al.* (16) for the Jen1 lactate permease. We went on to examine the effect of Snf1 overexpression, which we have shown increases 14-3-3 binding to Rod1. We observed a statically significant reduction in the percentage of the Rod1-Hxt6 BiFC signal present at plasma membrane at all three time points examined (p values < 0.001). Similar results were observed in cells overexpressing *BMH2*.

Our results suggest that either *SNF1* or *BMH2* overexpression partially impedes the plasma membrane localization of the Rod1-Hxt6 complex, which may reduce Hxt6 degradation by decreasing the efficiency of its ubiquitylation and subsequent entrance into the ESCRT pathway. This hypothesis is supported by experiments where we monitored the amount of Hxt6 accumulation by Western blotting (Fig. 9). We observe a time-dependent decrease in the amount of Hxt6-GFP in the wild type cells upon glucose addition, in agreement with a previous report (11). However, in strains overexpressing *SNF1* or *BMH2*, the disappearance of the Hxt6-GFP signal is delayed. These results with Hxt6 are consistent with the model proposed for Jen1 regulation, in which 14-3-3 protein binding would reduce Rod1-mediated Hxt6 ubiquitylation at the plasma membrane by Rsp5 (16).

Discussion

Correct regulation of the cohort of proteins capable of transporting nutrients and ions across the plasma membrane is crucial for proper adaptation to changing environmental conditions. Ubiquitylation plays an important role in this dynamic process in yeast, as well as in mammals and plants (1). In the case of yeast and mammals, HECT family E3 ubiquitin ligases, like Rsp5 (yeast) and Nedd4.2 (mammalian), have been shown to specifically target plasma membrane transport proteins. This ubiquitylation event participates in the sorting of these transporters to the degradative organelle (vacuole or lysosome) via the ESCRT pathway, thus facilitating their removal from the plasma membrane (reviewed in Ref. 25).

The yeast E3 ubiquitin ligase Rsp5 has been implicated in the down-regulation of a large number of diverse transporters (reviewed in Ref. 6). The recognition of such a variety of transporters requires the use of adaptor proteins, such as those belonging to the ART family. Most of these proteins contain (L/P)P*X*Y motifs that interact with the WW domains of Rsp5 and also arrestin-like domains, which have been proposed to mediate transporter recognition. Post-translational modification of these adaptor proteins provides another level of possible regulation in response to environmental changes. Several examples have been reported in the literature, such as the nitrogen-dependent regulation of Ldb19 (Art1) by the TOR-dependent Npr1 protein kinase and the carbon source-dependent regulation of Rod1 (Art4) by the Snf1 kinase (12, 16, 19). This latter case was shown to be involved in the regulation of the Jen1 lactate transporter, the Ste2 pheromone receptor, and the Hxt1 and Hxt3 hexose permeases (15–17).

In this report, we provide evidence showing that the regulatory network involving Snf1 and Rod1 is also involved in regulating the high affinity glucose transporter, Hxt6 (Fig. 10). We have mapped the physical interaction between these proteins, showing that the regulatory domain of Snf1 interacts with the N-terminal half of Rod1, which contains the arrestin-like domain. Our data also support and expand upon the role played by the 14-3-3 isoform, Bmh2 in the regulation of Rsp5 adaptor proteins. We show that in addition to Rod1, many other ART family proteins bind to Bmh2, thus suggesting a more general role for 14-3-3 proteins in the regulation of Rsp5-dependent transporter down-regulation. Further studies are required to

FIGURE 6. **Visualization of the Rod1-Hxt6 complex *in vivo* using bimolecular fluorescence complementation.** The *HXT6-VC*::*HIS3* strain was transformed with the *ROD1*-VN or the empty plasmid, and the wild type strain was co-transformed with the VC empty plasmid and the *ROD1*-VN, as indicated. The cells were grown to mid-log phase in raffinose medium. *A*, images of the BiFC fluorescence and the overlay with the transmitted light are shown. *B* and *C*, the *HXT6-VC*::*HIS3* strain expressing *ROD1*-VN was co-transformed with the endocytic vesicle marker DsRed-FYVE (*B*) or the TGN marker DsRed-Sec7 (*C*). Strains were grown to mid-log phase in raffinose medium and transferred to raffinose (*RAF*) or glucose (*GLU*) medium without methionine for 30 min to induce the expression of Rod1. The cells were visualized by confocal microscopy as indicated under "Experimental Procedures." *D*, the *HXT6-VC*::*HIS3* strain expressing *ROD1*-VN was grown to mid-log phase in raffinose medium, incubated with 2 μg/ml FM4-64 for 60 min, washed, resuspended in glucose medium without methionine, and visualized by confocal microscopy 60 min later. Representative cells are shown. Identical results were obtained for at least two independent transformants and in at least two experiments. *E*, the plasma membrane fluorescence/internal fluorescence ratio was calculated from the data described in *B* and *C* (a total of 126 untreated and 88 treated cells were quantified). The *horizontal midline* represents the median, and the *box* depicts the upper and lower quartiles. The *whiskers* denote the maximal and minimal fluorescence intensities (p value < 0.001).

define conditions under which these interactions will be physiologically relevant. Interestingly, an isoform of mammalian 14-3-3 has also been shown to regulate the Nedd4.2 E3 ubiquitin ligase (20, 21), although in this case the binding between these proteins has been reported to be direct and not via adaptor proteins, as in yeast.

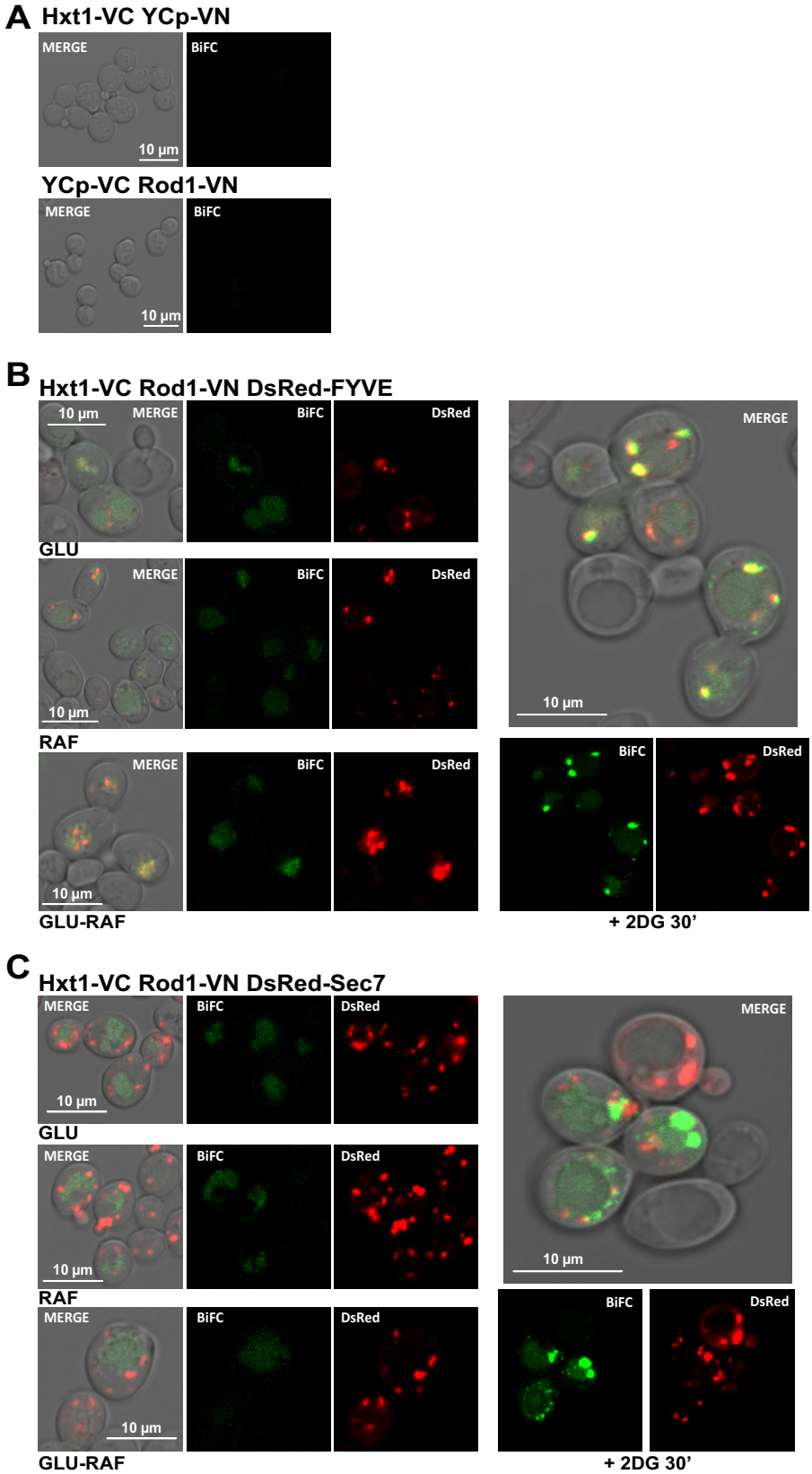

Although several reports have shown physical interactions between ART family members and specific transporter proteins biochemically (9, 10), our data provide the *in vivo* demonstration of this class of interactions. Importantly, using the BiFC technique, we observe the interaction between Rod1 and both Hxt6 and Hxt1 and show plasma membrane or endocytic vesicle accumulation for the Rod1-Hxt6 and Rod1-Hxt1 complexes, respectively. These data support the proposed model in which Rsp5 adaptor proteins would recruit the E3 ubiquitin ligase to the transporter under appropriate conditions to correctly and specifically mediate their down-regulation. Rod1 was proposed to interact with Jen1 at the TGN upon glucose treatment of lactate grown cells (26). We did not observe the formation of the Rod1-Hxt6 or Rod1-Hxt1 complexes in this organelle under the tested conditions. Our results indicate that Rod1 interacts with different cargo proteins in different subcellular locations in response to different stimuli. Therefore, this may explain the differences observed as compared with the Jen1 lactate transporter, although we cannot discard a transient interaction at this organelle, which was not detected at the time points examined (15 intervals from 15 to 90 min).

We also show that overexpression of either Snf1 or Bmh2 reduces the percentage of the Rod1-Hxt6 complex found at the plasma membrane, shedding light on the mechanism of action. In agreement with the model proposed by Becuwe *et al.* (16), both Snf1 and Bmh2 act as negative regulators of Rod1, not only in the case of the Jen1 lactate transporter but also in the case of the high affinity Hxt6 glucose permease. Here, we show that both Snf1 and Bmh2 associate with the N-terminal, arrestin-like domain containing fragment of Rod1. It was previously reported that the stability of the Rod1-Rsp5 complex is not altered by changes in carbon source (16). However, Rod1 ubiquitylation occurs upon disassociation of the Rod1-Bmh2 complex. Upon addition of glucose, which has been shown to lead to the down-regulation of Hxt6, the Hxt6-Rod1 complex (presumably containing Rsp5, but not Bmh2 or Snf1) accumulates at the plasma membrane, thus facilitating Hxt6 ubiquitylation and subsequent degradation in the vacuole via the ESCRT pathway.

The ART family of proteins shows structural homology to the mammalian α-arrestins (reviewed in Refs. 8 and 27). Very interestingly, α-arrestins have been shown to be involved in glucose homeostasis. Mouse models lacking the Tnxip α-arrestin gene show low insulin levels and low blood glucose, especially under fasting conditions (28–30). Knockdown experiments reducing Txnip expression show a marked increase in glucose uptake in an insulin-responsive cell model (31), consistent with the results presented here for the homologous yeast system. Glucose transporter levels were not tested in this study, and available data for the Txnip knock-out models have yet to document a change in glucose transporter levels (32, 33). However, the amount of plasma membrane-localized glucose transporters in key target tissues has not been rigorously tested. On the other hand, recently Txnip was shown to be phosphorylated by the AMP kinase and to bind to the GLUT1 transporter, mediating its internalization in cell culture model systems (34). However, a role for ubiquitylation of GLUT1 was not explored in this report. Moreover, overexpression of either Txnip or the related Arrdc4 is capable of reducing glucose uptake in cell culture models, in agreement with the proposed model (35). However, in this case, the (L/P)P*X*Y motifs that would bind to the WW domains of Rsp5-related E3 ubiquitin ligases are not required. Thus, it is possible that the underlying mechanisms of these evolutionarily diverse regulatory systems are different. However, there are clear parallels between these two signaling networks, and unraveling the molecular basis for hexose transporter regulation in yeast will contribute to the study of these key contributors to mammalian glucose homeostasis.

Experimental Procedures

The *S. cerevisiae* strains used in this work are listed in Table 1. The THY.AP4 strain was used for yeast two-hybrid analyses (36). YPD contained 2% peptone, 1% yeast extract, and 2% glucose (or 2% raffinose, YPRaf). Minimal yeast (MY) medium supplemented with the indicated carbon source was prepared as described (37). SD medium contained 2% glucose, 0.7% yeast nitrogen base (Difco) without amino acids, 50 mM succinic acid adjusted to pH 5.5 with Tris, and the amino acids and purine and pyrimidine bases required by the strains. LG medium is identical to the SD medium except that a mixture of 0.05% glucose, 2% glycerol, 2% galactose, and 2% ethanol was used as the carbon source. Growth assays were performed on solid medium by spotting serial dilutions of saturated cultures onto plates with the indicated composition.

Plasmids and Genomic Integrations—The open reading frames encoding the nine ART family members were amplified by PCR using specific primers containing appropriate restriction sites for the in-frame fusion in the pACT2 plasmid (Clontech). The Rod1-AD fusions were made by amplifying the coding sequence corresponding to base pairs 1–1185 and 1186–2511 using specific primers containing NcoI and SacI sites for cloning into pACT2. The SNF1 point mutants and *SNF1* and *BMH2* plasmids with LexA fusions were kindly provided by Dr. Pascual Sanz (Biomedical Institute of Valencia, Consejo Superior de Investigaciones Científicas) (23, 38). For co-immunoprecipitation experiments, *ROD1* was expressed from the pIC-Trp multicopy plasmid (DualSystems AG) cloned to maintain the in-frame fusion of the V5 epitope and *HXT6* was cloned into the HA epitope-containing pNTrp vector (DualSystems AG). All constructs were confirmed by sequencing. The plasmid-borne version of Rod1-VN and Hxt1-VC for BiFC experiments were constructed by homologous recombination in yeast using the pUG34-VC and pUG35-VN plasmids (39).

FIGURE 7. **Rod1 interacts with Hxt1 in endocytic vesicles upon 2-deoxyglucose treatment.** The wild type strain was transformed with plasmids encoding Hxt1-VC, Rod1-VN, or the corresponding empty vector controls as indicated. The cells were grown to mid-log phase in glucose medium. *A*, images of the BiFC fluorescence and the overlay with transmitted light are shown. *B* and *C*, the Hxt1-VC/Rod1-VN strain was co-transformed with the endocytic vesicle marker DsRed-FYVE (*B*) or the TGN marker DsRed-Sec7 (*C*). Strains were grown in glucose or raffinose containing medium and, where indicated, shifted to raffinose medium or treated with 2-deoxyglucose (0.2%) for 30 min. Representative confocal images are shown. In the *left set* of *panels* in *B* and *C*, the *far-left images* show the overlay, and the *middle* and *right panels* show the BiFC and DsRed channels, respectively. Treatments are indicated below each set of panels. Similar results were observed in at least two independent transformants.

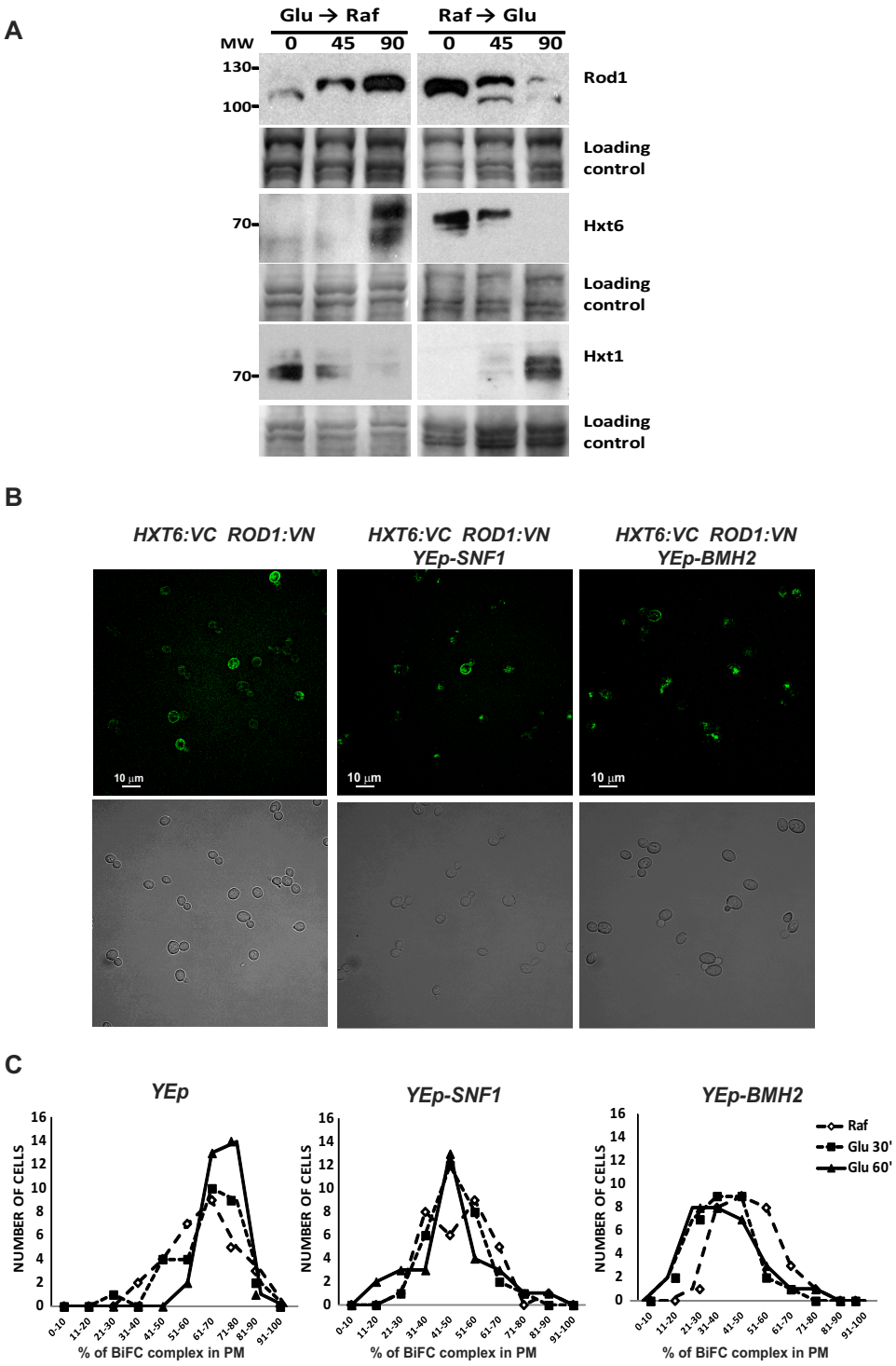

FIGURE 8. **Dynamic regulation of Rod1 and the Rod1-Hxt6 complex in response to changes in carbon source and signaling proteins.** *A*, protein accumulation of Rod1, Hxt6, and Hxt1 in response to carbon source. Strains containing genomic insertions of GFP were grown as indicated and processed for protein extraction and immunodetection using the α-GFP antibody. *B*, the indicated genomically integrated BiFC strains, generated as described under "Experimental Procedures," were grown in raffinose-containing medium (*Raf*) to the end of the log phase and analyzed by confocal microscopy to determine the presence and the subcellular localization of the Rod1-Hxt6 interaction by bimolecular fluorescence complementation. Representative images of samples 60 min after glucose (*Glu*) addition are shown. *C*, the strains described in *B* were grown in raffinose-containing MY medium and treated for the indicated times with glucose (final concentration, 2%). 30 individual cells were analyzed for each condition using the ImageJ software to determine the percentage of fluorescence intensity associated to the plasma membrane. The data were processed as described under "Experimental Procedures." The graphs represent the number of cells containing the indicated percentage of BiFC signal at the plasma membrane. The differences between the WT *versus SNF1* and the WT *versus BMH2* distributions were statistically significant (p value < 0.001) at all three time points, as assessed by nonparametric, two-tailed Mann-Whitney U tests. Similar results were observed in two separate experiments.

For genomic integration of the Venus fluorescent protein, fragments (VC or VN) were fused in-frame to the C terminus of the *HXT6* or *ROD1* coding sequences by transforming the BY4741 strain with PCR-derived fragments generated from the pFA6a-VC155-*HIS3MX6* plasmid (for *HXT6*) or the pFA6a-VN173-kanMX6 plasmid (for *ROD1*) (40). Correct insertion was confirmed by genomic PCR of candidate clones using appropriate primers. Negative controls for BiFC fluorescence were carried out using the single transformants (*HXT6*-VC::*HIS3* or *ROD1*-VN::kanMX transformed with the appropriate centromeric plasmids (pUG34-VC or pUG35-VN) expressing only the VC or VN fragments, respectively. No fluorescence was detected in either case (Figs. 6*A* and 7*A*). To integrate the GFP coding sequence at the C terminus of *HXT6*, *HXT1*, and *ROD1*, the GFP::*HIS3* module was amplified by PCR from the pFA6a-GFP(S65T)-*HIS3MX6* vector (41) using chimeric primers containing 20 bp corresponding to the GFP::*HIS3* module and 45 bp corresponding to the coding sequence immediately upstream and downstream of the STOP codon required for correct recombination. Recombinants were confirmed by sequencing PCR products that were amplified from genomic DNA using a forward primer 50 bp upstream of the STOP codon and a

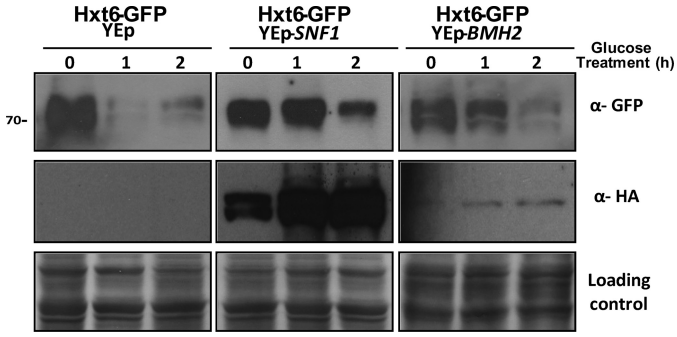

FIGURE 9. **Overexpression of either *SNF1* or *BMH2* delays the glucose-induced degradation of Hxt6.** The indicated plasmids were transformed into the *HXT6*-GFP::*HIS3* strain. These strains were grown and treated as indicated and processed for protein extraction and immunodetection. The α-GFP antibody detects the Hxt6-GFP fusion, and the α-HA antibody detects the Snf1-HA and Bmh2-HA fusions. The Snf1-HA and Bmh2 fusions migrate at ~80 and 45 kDa, respectively.

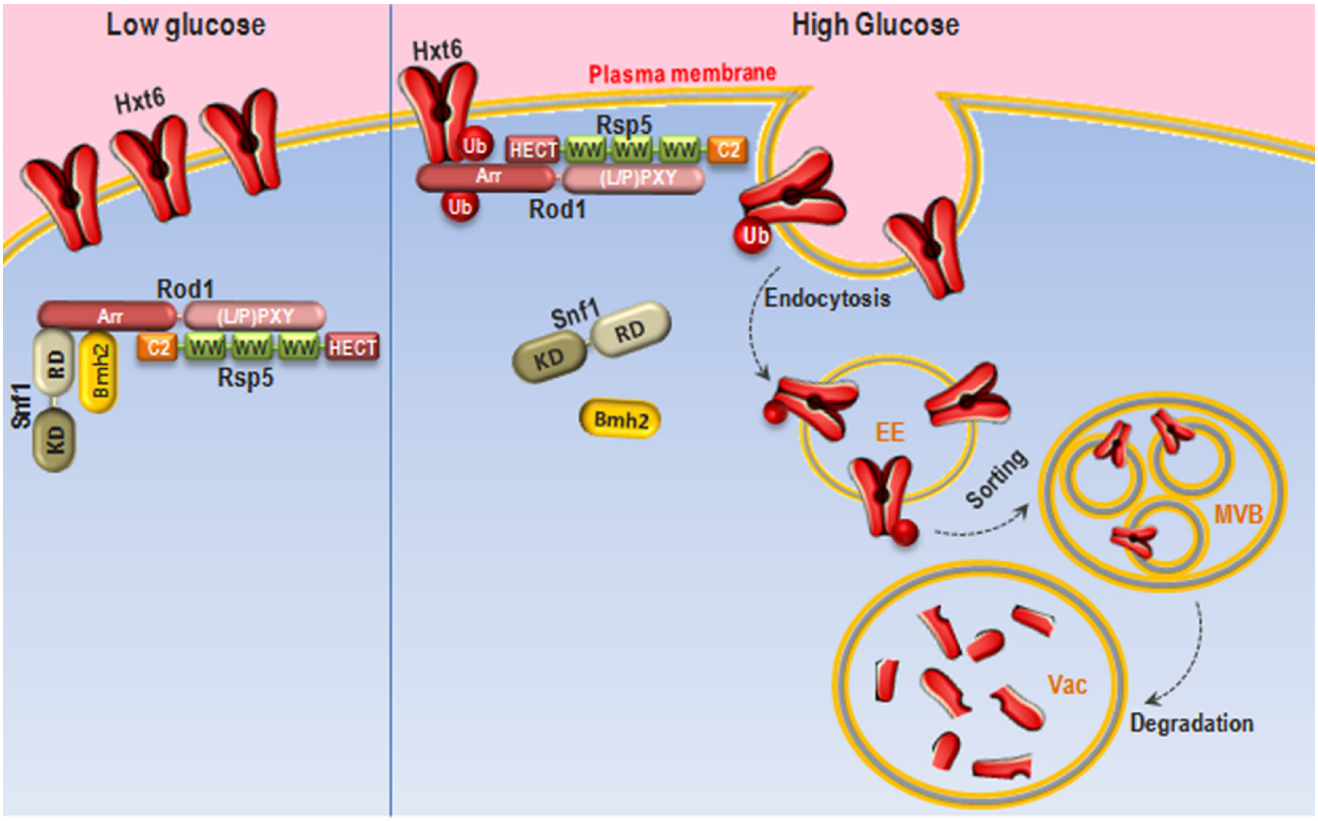

FIGURE 10. **Working model for Hxt6 regulation by the Rod1-Snf1–14-3-3 signaling pathway.** The 14-3-3 protein Bmh2 and the regulatory domain of Snf1 associate with the arrestin-like domain of Rod1. Rod1 forms a complex with Hxt6 at the plasma membrane, which facilitates its degradation upon glucose addition. Increased levels of Snf1 or Bmh2 reduce this association and delay Hxt6 degradation, presumably by reducing the efficiency of Rsp5-dependent ubiquitylation of the permease. *MVB*, multivesicular body; *EE*, early endosome; *Vac*, vacuole; *Arr*, arrestin-like domain; *KD*, kinase domain; *RD*, regulatory domain.

TABLE 1

Relevant genotypes of the strains used in this study

Strain	Relevant genotype	Reference
BY4741	Mata *ura3-0 leu2-0 his3-1 met15-0*	EUROSCARF
BY4741 *HXT6-GFP*	*HXT6-GFP::HIS3*	This study
BY4741 *HXT1-GFP*	*HXT1-GFP::HIS3*	This study
BY4741 *ROD1-GFP*	*ROD1-GFP::HIS3*	This study
BY4741 *HXT6-VC ROD1-VN*	*HXT6-VC::HIS3 ROD1-VN*::KanMX	This study
THY.AP4	*MATa ura3 leu2 lexA::lacZ::trp1 lexA::HIS3 lexA::ADE2*	Ref. 36

reverse primer 100 bp downstream of the *HIS3* start codon. The DsRed-FYVE endosomal marker and the Sec7-DsRed TGN marker were kindly provided by the laboratory of Dr. Kai Simons (24). The DsRed-FYVE construct employed here was generated from the DsRed-FYVE^{EEA1} fusion previously described, which is a phosphatidylinositol 3-phosphate-binding domain found on endosomal membranes (42).

Co-immunoprecipitation and Protein Analysis—Protein extracts, cross-linking, co-immunoprecipitation procedures, and immunoblot analyses were performed as described (43). The following antibodies were employed: α-GFP, high affinity α-HA and α-V5 (Roche), α-LexA (Abcam), α-HA (Covance), α-mouse IgG, and α-rabbit IgG conjugated to HRP (Amersham Biosciences).

Confocal Microscopy—Fluorescence images were obtained for live cells grown to the exponential phase in minimal medium using either the Zeiss 780 confocal microscope with excitation at 488 nm and detection at 510–550 nm for GFP (objective: plan-apochromat 40×/1.3 OIL DIC M27, Zeiss ZEN 2012 software) or the Zeiss LSM 5 Exciter-AxioImager M1 confocal microscope with excitation at 514 nm and detection at 520–570 nm for bimolecular fluorescence complementation experiments. For co-localization experiments and FM4-64 detection, sequential acquisition of DsRed signals was carried out with excitation at 561 nm and detection at 565–700 nm. Quantification of the cellular fluorescence distribution was carried out using the ImageJ software. Briefly, cells for each condition were randomly selected, and the fluorescence intensities for the whole cell and the cell interior (just inside the plasma membrane) were determined using the original cell contour and the same contour reduced by 5 pixels. Using these data (integrated density), the plasma membrane/internal fluorescence ratio or the percentage of total fluorescence associated with the plasma membrane was calculated for each individual cell (total fluorescence − internal fluorescence = plasma membranefluorescence;plasmamembranefluorescence/totalfluorescence × 100 = percentage of plasma membrane fluorescence). Statistical analysis of the data was performed with the IBM SPSS software package. To assess the statistical significance of the data in Fig. 8, nonparametric, two-tailed Mann-Whitney U tests were used.

β-Galactosidase Assays—Yeast cells transformed with the indicated plasmids were grown selectively in SD medium and then diluted in YPD. The cells were grown to exponential phase and then harvested by centrifugation (3000 rpm for 5 min). β-Galactosidase activity was determined as described elsewhere and represented as β-galactosidase activity units (44). The data are the mean from three independent transformants, each one measured in triplicate. *Error bars* represent the standard deviation.

Author Contributions—A. F.-B., E. D., and V. L.-T. designed and performed the experiments shown in Figs. 1–3. V. L.-T. designed and performed the experiments shown in Figs. 4, 5, 8, and 9. G. P. v. H. designed, performed, and analyzed the experiments shown in Fig. 8 and participated in the preparation of the manuscript. A. F. B. and A. A.-A. designed and performed the experiments shown in Figs. 6 and 7. L. Y. conceived and coordinated the study, prepared the figures, and wrote the paper. All authors reviewed the results and approved the final version of the manuscript.

Acknowledgments—We thank B. Romartínez and J. Delás for valuable technical assistance, Drs. Mª Carmen Marqués, Cecilia Primo, Purificación Lisón, and María Pilar López-Gresa for helpful discussions and Drs. Kai Simons and Pascual Sanz for plasmids.

References

1. Mulet, J. M., Llopis-Torregrosa, V., Primo, C., Marqués, M. C., and Yenush, L. (2013) Endocytic regulation of alkali metal transport proteins in mammals, yeast and plants. *Curr. Genet.* **59,** 207–230
2. Hein, C., Springael, J. Y., Volland, C., Haguenauer-Tsapis, R., and André, B. (1995) NPI1, an essential yeast gene involved in induced degradation of Gap1 and Fur4 permeases, encodes the Rsp5 ubiquitin-protein ligase. *Mol. Microbiol.* **18,** 77–87
3. Babst, M., Katzmann, D. J., Estepa-Sabal, E. J., Meerloo, T., and Emr, S. D. (2002) Escrt-III: an endosome-associated heterooligomeric protein complex required for mvb sorting. *Dev. Cell* **3,** 271–282
4. Babst, M., Katzmann, D. J., Snyder, W. B., Wendland, B., and Emr, S. D. (2002) Endosome-associated complex, ESCRT-II, recruits transport machinery for protein sorting at the multivesicular body. *Dev. Cell* **3,** 283–289
5. Katzmann, D. J., Babst, M., and Emr, S. D. (2001) Ubiquitin-dependent sorting into the multivesicular body pathway requires the function of a conserved endosomal protein sorting complex, ESCRT-I. *Cell* **106,** 145–155
6. Lauwers, E., Erpapazoglou, Z., Haguenauer-Tsapis, R., and André, B. (2010) The ubiquitin code of yeast permease trafficking. *Trends Cell Biol.* **20,** 196–204
7. Lin, C. H., MacGurn, J. A., Chu, T., Stefan, C. J., and Emr, S. D. (2008) Arrestin-related ubiquitin-ligase adaptors regulate endocytosis and protein turnover at the cell surface. *Cell* **135,** 714–725
8. Aubry, L., and Klein, G. (2013) True arrestins and arrestin-fold proteins: a structure-based appraisal. *Prog. Mol. Biol. Transl. Sci.* **118,** 21–56
9. Hatakeyama, R., Kamiya, M., Takahara, T., and Maeda, T. (2010) Endocytosis of the aspartic acid/glutamic acid transporter Dip5 is triggered by substrate-dependent recruitment of the Rsp5 ubiquitin ligase via the arrestin-like protein Aly2. *Mol. Cell. Biol.* **30,** 5598–5607
10. Nikko, E., Sullivan, J. A., and Pelham, H. R. (2008) Arrestin-like proteins mediate ubiquitination and endocytosis of the yeast metal transporter Smf1. *EMBO Rep.* **9,** 1216–1221
11. Nikko, E., and Pelham, H. R. (2009) Arrestin-mediated endocytosis of yeast plasma membrane transporters. *Traffic* **10,** 1856–1867
12. MacGurn, J. A., Hsu, P. C., Smolka, M. B., and Emr, S. D. (2011) TORC1 regulates endocytosis via Npr1-mediated phosphoinhibition of a ubiquitin ligase adaptor. *Cell* **147,** 1104–1117
13. Merhi, A., and André, B. (2012) Internal amino acids promote Gap1 permease ubiquitylation via TORC1/Npr1/14-3-3-dependent control of the Bul arrestin-like adaptors. *Mol. Cell. Biol.* **32,** 4510–4522
14. O'Donnell, A. F., Huang, L., Thorner, J., and Cyert, M. S. (2013) A calcineurin-dependent switch controls the trafficking function of α-arrestin Aly1/Art6. *J. Biol. Chem.* **288,** 24063–24080
15. O'Donnell, A. F., McCartney, R. R., Chandrashekarappa, D. G., Zhang, B. B., Thorner, J., and Schmidt, M. C. (2015) 2-Deoxyglucose impairs *Saccharomyces cerevisiae* growth by stimulating Snf1-regulated and α-arrestin-mediated trafficking of hexose transporters 1 and 3. *Mol. Cell. Biol.* **35,** 939–955
16. Becuwe, M., Vieira, N., Lara, D., Gomes-Rezende, J., Soares-Cunha, C., Casal, M., Haguenauer-Tsapis, R., Vincent, O., Paiva, S., and Léon, S. (2012) A molecular switch on an arrestin-like protein relays glucose signaling to transporter endocytosis. *J. Cell Biol.* **196,** 247–259
17. Alvaro, C. G., Aindow, A., and Thorner, J. (2016) Differential phosphorylation provides a switch to control how α-arrestin Rod1 down-regulates mating pheromone response in *Saccharomyces cerevisiae*. *Genetics* **203,** 299–317
18. Alvaro, C. G., O'Donnell, A. F., Prosser, D. C., Augustine, A. A., Goldman, A., Brodsky, J. L., Cyert, M. S., Wendland, B., and Thorner, J. (2014) Specific α-arrestins negatively regulate *Saccharomyces cerevisiae* pheromone

response by down-modulating the G-protein-coupled receptor Ste2. *Mol. Cell. Biol.* **34,** 2660–2681
19. Shinoda, J., and Kikuchi, Y. (2007) Rod1, an arrestin-related protein, is phosphorylated by Snf1-kinase in *Saccharomyces cerevisiae*. *Biochem. Biophys. Res. Commun.* **364,** 258–263
20. Ichimura, T., Yamamura, H., Sasamoto, K., Tominaga, Y., Taoka, M., Kakiuchi, K., Shinkawa, T., Takahashi, N., Shimada, S., and Isobe, T. (2005) 14-3-3 proteins modulate the expression of epithelial Na^+ channels by phosphorylation-dependent interaction with Nedd4-2 ubiquitin ligase. *J. Biol. Chem.* **280,** 13187–13194
21. Bhalla, V., Daidié, D., Li, H., Pao, A. C., LaGrange, L. P., Wang, J., Vandewalle, A., Stockand, J. D., Staub, O., and Pearce, D. (2005) Serum- and glucocorticoid-regulated kinase 1 regulates ubiquitin ligase neural precursor cell-expressed, developmentally down-regulated protein 4–2 by inducing interaction with 14-3-3. *Mol. Endocrinol.* **19,** 3073–3084
22. Sanz, P., Ludin, K., and Carlson, M. (2000) Sip5 interacts with both the Reg1/Glc7 protein phosphatase and the Snf1 protein kinase of *Saccharomyces cerevisiae*. *Genetics* **154,** 99–107
23. Jiang, R., and Carlson, M. (1996) Glucose regulates protein interactions within the yeast SNF1 protein kinase complex. *Genes Dev.* **10,** 3105–3115
24. Proszynski, T. J., Klemm, R. W., Gravert, M., Hsu, P. P., Gloor, Y., Wagner, J., Kozak, K., Grabner, H., Walzer, K., Bagnat, M., Simons, K., and Walch-Solimena, C. (2005) A genome-wide visual screen reveals a role for sphingolipids and ergosterol in cell surface delivery in yeast. *Proc. Natl. Acad. Sci. U.S.A.* **102,** 17981–17986
25. MacGurn, J. A., Hsu, P.-C., and Emr, S. D. (2012) Ubiquitin and membrane protein turnover: from cradle to grave. *Annu. Rev. Biochem.* **81,** 231–259
26. Becuwe, M., and Léon, S. (2014) Integrated control of transporter endocytosis and recycling by the arrestin-related protein Rod1 and the ubiquitin ligase Rsp5. *Elife* **3,** 03307
27. Alvarez, C. E. (2008) On the origins of arrestin and rhodopsin. *BMC Evol. Biol.* **8,** 222
28. Chutkow, W. A., Patwari, P., Yoshioka, J., and Lee, R. T. (2008) Thioredoxin-interacting protein (Txnip) is a critical regulator of hepatic glucose production. *J. Biol. Chem.* **283,** 2397–2406
29. Sheth, S. S., Castellani, L. W., Chari, S., Wagg, C., Thipphavong, C. K., Bodnar, J. S., Tontonoz, P., Attie, A. D., Lopaschuk, G. D., and Lusis, A. J. (2005) Thioredoxin-interacting protein deficiency disrupts the fasting-feeding metabolic transition. *J. Lipid Res.* **46,** 123–134
30. Bodnar, J. S., Chatterjee, A., Castellani, L. W., Ross, D. A., Ohmen, J., Cavalcoli, J., Wu, C., Dains, K. M., Catanese, J., Chu, M., Sheth, S. S., Charugundla, K., Demant, P., West, D. B., de Jong, P., and Lusis, A. J. (2002) Positional cloning of the combined hyperlipidemia gene Hyplip1. *Nat. Genet.* **30,** 110–116
31. Parikh, H., Carlsson, E., Chutkow, W. A., Johansson, L. E., Storgaard, H., Poulsen, P., Saxena, R., Ladd, C., Schulze, P. C., Mazzini, M. J., Jensen, C. B., Krook, A., Björnholm, M., Tornqvist, H., Zierath, J. R., Ridderstråle, M., Altshuler, D., Lee, R. T., Vaag, A., Groop, L. C., and Mootha, V. K. (2007) TXNIP regulates peripheral glucose metabolism in humans. *PLoS Med.* **4,** e158
32. Yoshioka, J., Imahashi, K., Gabel, S. A., Chutkow, W. A., Burds, A. A., Gannon, J., Schulze, P. C., MacGillivray, C., London, R. E., Murphy, E., and Lee, R. T. (2007) Targeted deletion of thioredoxin-interacting protein regulates cardiac dysfunction in response to pressure overload. *Circ. Res.* **101,** 1328–1338
33. Andres, A. M., Ratliff, E. P., Sachithanantham, S., and Hui, S. T. (2011) Diminished AMPK signaling response to fasting in thioredoxin-interacting protein knockout mice. *FEBS Lett.* **585,** 1223–1230
34. Wu, N., Zheng, B., Shaywitz, A., Dagon, Y., Tower, C., Bellinger, G., Shen, C. H., Wen, J., Asara, J., McGraw, T. E., Kahn, B. B., and Cantley, L. C. (2013) AMPK-dependent degradation of TXNIP upon energy stress leads to enhanced glucose uptake via GLUT1. *Mol. Cell* **49,** 1167–1175
35. Patwari, P., Chutkow, W. A., Cummings, K., Verstraeten, V. L., Lammerding, J., Schreiter, E. R., and Lee, R. T. (2009) Thioredoxin-independent regulation of metabolism by the alpha-arrestin proteins. *J. Biol. Chem.* **284,** 24996–25003
36. Paumi, C. M., Menendez, J., Arnoldo, A., Engels, K., Iyer, K. R., Thaminy, S., Georgiev, O., Barral, Y., Michaelis, S., and Stagljar, I. (2007) Mapping protein-protein interactions for the yeast ABC transporter Ycf1p by integrated split-ubiquitin membrane yeast two-hybrid analysis. *Mol. Cell* **26,** 15–25
37. Zonneveld, B. J. (1986) Cheap and simple yeast media. *J. Microbiol. Methods* **4,** 287–291
38. Mayordomo, I., Regelmann, J., Horak, J., and Sanz, P. (2003) *Saccharomyces cerevisiae* 14-3-3 proteins Bmh1 and Bmh2 participate in the process of catabolite inactivation of maltose permease. *FEBS Lett.* **544,** 160–164
39. Zahrádka, J., van Heusden, G. P., and Sychrová, H. (2012) Yeast 14-3-3 proteins participate in the regulation of cell cation homeostasis via interaction with Nha1 alkali-metal-cation/proton antiporter. *Biochim. Biophys. Acta* **1820,** 849–858
40. Sung, M. K., and Huh, W. K. (2007) Bimolecular fluorescence complementation analysis system for in vivo detection of protein-protein interaction in *Saccharomyces cerevisiae*. *Yeast* **24,** 767–775
41. Longtine, M. S., McKenzie, A., 3rd, Demarini, D. J., Shah, N. G., Wach, A., Brachat, A., Philippsen, P., and Pringle, J. R. (1998) Additional modules for versatile and economical PCR-based gene deletion and modification in *Saccharomyces cerevisiae*. *Yeast* **14,** 953–961
42. Burd, C. G., and Emr, S. D. (1998) Phosphatidylinositol(3)-phosphate signaling mediated by specific binding to RING FYVE domains. *Mol. Cell* **2,** 157–162
43. Yenush, L., Merchan, S., Holmes, J., and Serrano, R. (2005) pH-responsive, posttranslational regulation of the Trk1 potassium transporter by the type 1-related Ppz1 phosphatase. *Mol. Cell. Biol.* **25,** 8683–8692
44. Gaxiola, R., de Larrinoa, I. F., Villalba, J. M., and Serrano, R. (1992) A novel and conserved salt-induced protein is an important determinant of salt tolerance in yeast. *EMBO J.* **11,** 3157–3164

Regulation of the Yeast Hxt6 Hexose Transporter by the Rod1 α-Arrestin, the Snf1 Protein Kinase, and the Bmh2 14-3-3 Protein

Vicent Llopis-Torregrosa, Alba Ferri-Blázquez, Anna Adam-Artigues, Emilie Deffontaines, G. Paul H. van Heusden and Lynne Yenush

J. Biol. Chem. 2016, 291:14973-14985.
doi: 10.1074/jbc.M116.733923 originally published online June 3, 2016